Elsevier Editorial System(tm) for International Journal of Heat and Mass Transfer
Manuscript Draft

Manuscript Number: HMT-D-13-00189R1

Title: Effect of advanced surfaces on the ammonia absorption process with NH3/LiNO3 in a tubular bubble absorber

Article Type: Full Length Article

Keywords: Bubble absorber, advanced surfaces, tubular heat exchanger, ammonia; lithium nitrate.

Corresponding Author: Prof. Mahmoud Bourouis, Ph.D.

Corresponding Author's Institution: Rovira i Virgili University

First Author: Carlos Amaris, Ph.D. Student

Order of Authors: Carlos Amaris, Ph.D. Student; Mahmoud Bourouis, Ph.D.; Manel Vallès, Ph.D.

Abstract: An experimental study was conducted to investigate the effect of advanced surfaces on the ammonia absorption process in tubular bubble absorbers using NH3/LiNO3 as a working pair at operating conditions of interest for absorption chillers. The tubular bubble absorber is a vertical double-pipe heat exchanger in which absorption takes place in the inner tube. In order to compare the effect of surface enhancement, a smooth tube and an internally micro-finned tube were tested. The inner tube of the absorber is made of aluminium and has an outer diameter of 8.0 mm and the micro-finned tube has internal helical micro-fins measuring 0.3 mm in length. The effect of tube length on absorption was also studied using two tube lengths (1 and 3 m) and two tube diameters (8 and 9.5 mm).
Our results show that the absorption rate achieved with the micro-finned tube is up to 1.7 times higher than with the smooth tube at a solution mass flow rate of 40 kg.h-1. We also found that absorption mass flux increases when tube diameter is reduced and decreases when tube length is increased.

Effect of advanced surfaces on the ammonia absorption process with $NH_3/LiNO_3$ in a tubular bubble absorber

Carlos Amaris, Mahmoud Bourouis* and Manel Vallès

CREVER – Universitat Rovira i Virgili, Av. Països Catalans No. 26,

43007 Tarragona, Spain. *Corresponding author

ABSTRACT

An experimental study was conducted to investigate the effect of advanced surfaces on the ammonia absorption process in tubular bubble absorbers using $NH_3/LiNO_3$ as a working pair at operating conditions of interest for absorption chillers. The tubular bubble absorber is a vertical double-pipe heat exchanger in which absorption takes place in the inner tube. In order to compare the effect of surface enhancement, a smooth tube and an internally micro-finned tube were tested. The inner tube of the absorber is made of aluminium and has an outer diameter of 8.0 mm and the micro-finned tube has internal helical micro-fins measuring 0.3 mm in length. The effect of tube length on absorption was also studied using two tube lengths (1 and 3 m) and two tube diameters (8 and 9.5 mm).

Our results show that the absorption rate achieved with the micro-finned tube is up to 1.7 times higher than with the smooth tube at a solution mass flow rate of 40 $kg.h^{-1}$. We also found that absorption mass flux increases when tube diameter is reduced and decreases when tube length is increased.

Keywords: Bubble absorber, advanced surfaces, tubular heat exchanger, ammonia; lithium nitrate.

Highlights

- We conducted an experimental study on the intensification of the absorption process with $NH_3/LiNO_3$ mixture in a tubular bubble absorber.

- We compared the experimental results yielded by a tubular absorber using advanced and smooth surfaces.
- The maximum NH_3 absorption mass flux obtained with the advanced surface tube was approximately 1.7 times higher than the values achieved with the smooth tube.

Nomenclature

A	*heat transfer area*
C	*correction factor*
Cp	*heat capacity*
D	*diameter*
f	*friction factor*
F	*NH_3 absorption mass flux*
h	*heat transfer coefficient*
Km	*mass transfer coefficient*
k	*thermal conductivity*
LMTD	*Logarithmic Mean Temperature Difference*
LMXD	*Logarithmic Mean Concentration Difference*
$\dot{m}$	*mass flow rate*
Nu	*Nusselt number*
OD	*outer diameter*
Pr	*Prandtl number*
Q	*thermal load per unit of area*
Q_{AB}	*thermal load in the absorber*
Re	*Reynolds number*
U	*overall heat transfer coefficient*
V	*volumetric flow rate*
x	*NH_3 mass fraction in solution*

Subscripts:

AB	*absorber*
Al	*aluminium*
Cw	*cooling water*
Eq	*equilibrium*
In	*absorber inlet*
Inner	*inner diameter of the tube*
NH_3	*ammonia*
Out	*absorber outlet*

Outer *outer diameter of the tube*

Sol *solution of $NH_3/LiNO_3$*

Sat *saturation state*

Sub *subcooling*

TA *tubular Absorber*

o *outer tube*

Greek letters:

ΔT *temperature difference*

Δx *concentration difference*

ρ *density*

1. Introduction

The increasing costs of primary energy and growing interest in protecting the environment have promoted the use of absorption chillers driven by waste heat or solar thermal energy. Today, absorption refrigeration systems and heat pumps use H_2O/LiBr and NH_3/H_2O mixtures as working fluids. These working fluids have some drawbacks, such as crystallization and corrosion problems, low pressure operation for the H_2O/LiBr mixture and the need to rectify the refrigerant vapour at the desorber outlet for the NH_3/H_2O mixture. Due to the limitations of conventional working fluids, research is currently being done into new mixtures and the application of passive intensification techniques to improve absorption machines. Studies on absorption systems with $NH_3/LiNO_3$ have yielded interesting results that suggest this may be a promising working pair for absorption refrigeration cycles driven by low temperature heat sources [1-3]. The lack of crystallization means that refrigeration cycles with $NH_3/LiNO_3$ can be operated at high condensation temperatures, which in turn means that air-cooled condensers can be used. The cycle can be activated at lower generator temperatures than with NH_3/H_2O, and the refrigerant vapour leaving the generator does not require rectification [4-7], the primary drawback of NH_3/H_2O working fluid. Therefore, the advantages of this mixture are the simplicity of the cycle and a greater potential for solar cooling. Its drawback is its high viscosity, which is detrimental to heat and mass transfer processes, primarily in the absorber [6-9]. According to the available literature, absorption cooling prototypes initially designed to operate with the NH_3/H_2O working pair and loaded with an $NH_3/LiNO_3$ working pair have yielded poor experimental

results [7-9]. The authors of these experimental studies concluded that the main reason for this poor performance lies in the absorber because of the high viscosity of this mixture compared to NH_3/H_2O. These studies found that the high viscosity of $NH_3/LiNO_3$ diminished the performance predicted by thermodynamic models, and that this decreased performance was more pronounced at low cooling-water temperatures because of a dramatic increase in viscosity of the working fluid inside the absorber.

Based on the abovementioned studies, heat and mass transfer processes must be intensified inside the absorber of absorption refrigeration systems using an $NH_3/LiNO_3$ mixture. Higher heat and mass transfer coefficients would allow the heat exchanger size to be reduced or, what is even more interesting, the cycle driving temperature for solar cooling applications to be decreased and/or the heat sink temperature for the heat released in the absorber and condenser to be increased, thereby eliminating the need for wet cooling towers.

Absorption enhancement techniques are generally categorised into two methods: chemical and mechanical treatments [10]. The chemical treatment, which has been the subject of an extensive body of research, involves of the addition of small quantities of a surfactant that causes interfacial turbulence and leads to higher heat and mass transfer coefficients. Mechanical treatment includes both scratching the tube surface to increase surface roughness and the use of advanced surface tubes such as constant curvature tubes, fluted tubes and micro-finned tubes.

Among the most recent studies on the mechanical treatment of tubes to increase the absorption rate, Miller [11] measured the absorption rate and the heat transfer coefficient in a H_2O/LiBr horizontal tube absorber comparing several advanced surface tubes. The author also analysed the synergism of the effects of advanced surfaces and additives. The conclusion drawn from the study was that the improvement stemming from the mechanical mixing of advanced surfaces was not as effective as the enhancement induced by the chemical agitation of the additive, and that the synergistic effect was rather small. Park et al. [12] arrived at the same conclusion in their study on the effect of heat transfer additive and surface roughness of micro-scale hatched tubes on absorption performance in an H_2O/LiBr horizontal tube absorber. In a previous work on the same topic, Kim et al. [10] analysed the effect of the roughness of micro-scaled hatched tubes on wettability in an H_2O/LiBr falling film absorber and found that the wettability of micro-scale hatched tubes was higher than for smooth tubes.

Absorption studies with advanced surfaces include several research works with plate heat exchangers. Kang et al. [13] conducted experiments for the NH_3/H_2O falling film absorption process in a plate heat exchanger with enhanced surfaces such as an offset strip fin (OSF). The solution and vapour entered at the top of the plate heat exchanger and flowed downward. The coolant entered the test section from the bottom and flowed upward in the counter-current direction to the liquid solution flow. The authors examined the effects of liquid and vapour flow characteristics, inlet subcooling of the liquid flow and inlet concentration difference on heat and mass transfer performance and presented correlations for heat and mass transfer coefficients. Lee et al. [14] studied the effect of solution and vapour flow rates on a plate-type counter-current NH_3/H_2O bubble absorber. Three types of plates were tested: smooth plate, hair lined plate treated by laser, and plate treated with sand paper. Nusselt and Sherwood numbers were correlated as functions of solution Reynolds and gas Reynolds numbers to establish the solution and gas characteristics of the absorption rate. Recently, Cerezo et al. [15] carried out experimental studies using a corrugated three-channel plate heat exchanger as a bubble absorber and NH_3/H_2O as a working fluid. The coolant flowed inside the outer channels of the absorber while the weak solution flowed in counter-flow in the central channel. Vapour bubbles were injected at the inlet of the weak solution through a 1.7 mm orifice. The experimental data and predicted values of the absorber's thermal load and absorption mass flux from a theoretical model were compared at different operating conditions in terms of pressure drop, pressure, cooling-water and solution flow rates, solution concentration and cooling-water and solution temperatures.

Regarding the $NH_3/LiNO_3$ mixture, although Infante Ferreira [16] presented experimental results using this working pair in a vertical tubular bubble absorber, to our knowledge the only work available in the literature dealing with the use of advanced surfaces in an absorber with $NH_3/LiNO_3$ is a study recently published by Oronel et al. [17]. These authors carried out an experimental study on absorption processes with $NH_3/LiNO_3$ and $NH_3/(LiNO_3+H_2O)$ mixtures in a three-channel plate heat exchanger with L type corrugations. They performed a sensitivity analysis of the effects of the primary operating conditions such as weak solution inlet concentration and flow rate, and cooling-water inlet temperature and flow rate on absorber efficiency. Their results showed that for binary and ternary mixtures, the absorption mass flux, heat transfer coefficient, subcooling and mass transfer coefficient increase as the solution flow rate

increases. Moreover, empirical correlations for the solution Nusselt and Sherwood numbers are proposed on the basis of the experimental data collected.

The objective of this paper is to analyse the effect of advanced aluminium surfaces on the heat and mass transfer processes taking place inside the absorber, which is the most critical component in absorption refrigeration cycles. A $NH_3/LiNO_3$ mixture was used as the working pair due to its promising potential for solar cooling refrigeration applications.

Our experiments were performed in an experimental setup under operating conditions of interest for absorption chillers. The absorber tested is a double-pipe bubble absorber with an inner tube made of aluminium with an internal micro-finned surface.

2. Experimental test facility

Fig. 1 shows the experimental test facility used to study the absorption process in tubular bubble absorbers. This experimental test facility, initially built for the characterisation of plate heat exchangers as absorbers [15, 17], was modified and adapted to study the ammonia absorption process in tubular bubble absorbers. The facility allows operating parameters of interest to be monitored and controlled including solution and cooling-water flow rates, solution and cooling-water temperatures, ammonia concentration in the solution and operating pressure in the absorber.

The test facility consists of three circuits: the solution circuit, the cooling-water circuit, and the heating-water circuit. The solution circuit (dark and pea green lines) consists mainly of two stainless-steel tanks (ST1 and ST2), a magnetically coupled internal gear pump, a heat exchanger (SHE), a vapour-liquid separator (VLS) and the test section where the NH_3 absorption process takes place. The cooling-water circuit consists of a 5 kW heater (R2), a magnetic flow meter, a pump and a heat exchanger (HX1). Heat released by the absorption process is removed by the cooling-water circuit. The heating-water circuit consists of a 5 kW heater (R1), a pump and a magnetic flow meter. This circuit allows the solution to be heated to the required temperature before it enters the absorber.

In the solution circuit, the solution weak in refrigerant (pea green line) that has previously been heated in the heat exchanger (SHE) is pumped from the storage tank (ST1) to the bottom of the absorber (ABS), where it absorbs ammonia vapour in bubble mode fed from an ammonia bottle using a thin tube with an internal diameter of 1.7

mm. The ammonia vapor flow was controlled with a needle valve (NVA) and a mass flow controller (FC) located as shown in Fig. 1. In each experiment, the maximum ammonia absorption was obtained by measuring and controlling the density of the solution leaving the absorber.

The solution strong in refrigerant (dark green line) leaves the absorber at the top and flows to the VLS tank, and then the solution flows to tank ST2 where it is stored. Finally, the solution is sent to tank ST1 under the initial conditions of interest to start a new test.

Cooling-water and solution streams can be arranged in a co-current or counter-current configuration by manipulating a series of valves as shown in Fig. 1. In this study, the solution and ammonia vapour flowed in co-current and the cooling-water flowed in a counter-current configuration in relation to the solution and vapour streams.

Measuring instruments such as RTD temperature sensors (T), pressure transducers (P), magnetic flow meters (F) and Coriolis flow meters (C) were located in the experimental test facility as shown in Fig. 1. The density, temperature and mass flow rate of the weak and strong solutions were measured by Coriolis flow meters. In each experiment, once a steady-state regime was reached, measured data of the operating conditions were maintained and recorded for 10 to 20 minutes. Thermodynamic and transport properties of the $NH_3/LiNO_3$ mixture at the conditions under study were calculated using the correlations presented by Libotean et al. [18, 19]. Solution concentrations in ammonia at the absorber inlet and outlet were determined from the density and temperature values measured by the Coriolis flow meters using the density correlation reported by Libotean et al. [19].

2.1 Test section

A vertical tubular absorber was set in the test section of the experimental test facility used in this study. The tubular absorber consisted of a double-pipe heat exchanger with an inner tube made of aluminium, as shown in Fig. 2. The interior surface of the tube has helical micro-fins measuring 0.3 mm in height and a helix angle of 20º. The absorber was tested using a micro-finned tube with an exterior diameter of 8.0 mm and the results were compared with those previously achieved with an internally smooth tube. An additional micro-finned tube with an exterior diameter of 9.5 mm was also tested and compared with results from the 8-mm micro-finned tube. Finally, the tubular

absorber using the inner advanced surface tube was tested with two tube lengths (one and three metres in series). The total measured pressure drop of the studied configurations was documented. The main geometric characteristics of the absorber are given in Table 1. The interior diameter (internal equivalent diameter) was measured at the fin tip.

3. Absorber efficiency parameters

The parameters considered to assess absorber efficiency are defined here.

3.1 Absorption mass flux

Absorption mass flux (F_{AB}), which quantifies the capacity of the system to absorb ammonia vapour from the evaporator, is defined as the absorbed ammonia mass flow rate per unit of heat transfer area:

$$F_{AB} = \frac{\dot{m}_{NH3,Absorbed}}{A_{Exchange}} \tag{1}$$

where $A_{Exchange}$ is the heat exchange area (using the exterior diameter of the tube) for each case study and $\dot{m}_{NH3,absorbed}$ is calculated as:

$$\dot{m}_{NH3,Absorbed} = \dot{m}_{out} \cdot x_{out} - \dot{m}_{in} \cdot x_{in} \tag{2}$$

3.2 Heat transfer coefficient

The absorber thermal load is determined from the measured data on the water side:

$$Q_{AB} = \dot{m}_{Cw} \cdot Cp_{Cw} \cdot \left(T_{Cw,Out} - T_{Cw,In}\right) \tag{3}$$

The overall heat transfer coefficient U is given as:

$$U = \frac{Q_{AB}}{A_{Exchange} \cdot LMTD} \tag{4}$$

where *LMTD* is the standard definition of the logarithmic mean temperature difference involving solution and cooling-water temperatures at the inlet and outlet of the absorber. The solution heat transfer coefficient (h_{Sol_TA}) in the tubular absorber is obtained from:

$$\frac{1}{U \cdot D_{Outer}} = \frac{1}{h_{Sol\_TA} \cdot D_{Inner}} + \frac{Ln(D_{Outer} / D_{Inner})}{2 \cdot k_{Al}} + \frac{1}{D_{Outer} \cdot h_{Cw\_TA}} \tag{5}$$

The cooling-water heat transfer coefficient ($h_{Cw\text{-}TA}$) in the tubular absorber was determined using the well known Dittus-Boelter correlation:

The cooling-water heat transfer coefficient (h_{Cw}) in the tubular absorber was determined by using the Gnielinski´s correlation for the Nusselt number (Nu_{Cw}). This correlation has been proved valid for smooth tubes over a wide range of the Reynolds number including the transition region [20].

$$\mathrm{Nu}_{Cw} = \left[\frac{(f/8) \cdot (\mathrm{Re} - 1000) \cdot \mathrm{Pr}}{1 + 12.7(f/8)^{0.5}(\mathrm{Pr}^{2/3} - 1)} \right] \cdot C \tag{6}$$

where f is the friction factor obtained from the correlation developed by Petukhov [21]. C is the correction factor for flows in annular spaces, which was reported by Petukhov and Royzen [22] as a function of the ratio of diameters D_{outer} and $D_{inner,o}$:

$$C = 0.86 \left(\frac{D_{Outer}}{D_{inner,o}} \right)^{-0.16} \tag{7}$$

3.3 Mass transfer coefficient

The overall mass transfer coefficient was obtained as:

$$K_m = \frac{\dot{m}_{NH3,Absorbed}}{A_{Exchange} \cdot LMXD} \tag{8}$$

The logarithmic mean concentration difference (*LMXD*) expresses the nominal log-mean concentration difference along the absorber channel.

$$LMXD = \frac{\left(x_{Sat,Sol} \cdot \rho_{Sat,Sol} - x_{Sol} \cdot \rho_{Sol} \right)_{In} - \left(x_{Sat,Sol} \cdot \rho_{Sat,Sol} - x_{Sol} \cdot \rho_{Sol} \right)_{Out}}{\ln \dfrac{\left(x_{Sat,Sol} \cdot \rho_{Sat,Sol} - x_{Sol} \cdot \rho_{Sol} \right)_{In}}{\left(x_{Sat,Sol} \cdot \rho_{Sat,Sol} - x_{Sol} \cdot \rho_{Sol} \right)_{Out}}} \tag{9}$$

Saturation concentrations in Eq. (9) were calculated from measured temperatures and pressures values, using the correlations reported by Libotean et al. [18].

3.4 Degree of subcooling

The degree of subcooling of the solution at the absorber outlet (ΔT_{Sub}) indicates the degree of available absorption potential:

$$\Delta T_{Sub} = (T_{Sol,Eq,Out} - T_{Sol,Out}) \quad (10)$$

where $T_{Sol,Eq,Out}$ is the equilibrium solution temperature at the absorber pressure and actual outlet solution concentration.

3.5 Uncertainty propagation

Table 2 shows the uncertainty intervals of the calculated absorber efficiency parameters presented above taking into consideration a 95 % confidence interval. Uncertainties of calculated parameters were obtained using the method proposed in Technical Note 1297 of the National Institute of Standards and Technology Technical (NIST) and implemented in EES software (Taylor and Kuyatt [23]).

4. Experimental results and discussion

In this section, we present our experimental results for the main parameters for assessing the efficiency of a bubble absorber with an $NH_3/LiNO_3$ mixture. The results of the ammonia absorption process in a tubular heat exchanger with internal aluminium advanced surface were analysed and compared with the results achieved in a tubular absorber with smooth surfaces. Finally, as tube diameter and length are key parameters in the design of bubble absorbers, we carried out an experimental characterisation of the advanced surface tubular absorber with three tube lengths (1 and 3 metres in series) and two tube diameters (8 and 9.5 mm).

The operating conditions of interest for testing of the absorbers are shown in Table 3. These operating conditions were determined from a thermodynamic simulation of a single-effect absorption refrigeration cycle with $NH_3/LiNO_3$ at evaporation and

condensation/absorption temperatures of 5 ºC and 40 ºC, respectively. The tubular absorber with the different configurations was tested at the same operating conditions for the purpose of direct comparison.

4.1 Effect of advanced surfaces on absorber performance

Fig. 3 shows the NH_3 absorption mass flux, solution heat transfer coefficient, mass transfer coefficient and degree of subcooling as a function of the solution and cooling-water mass flows for the $NH_3/LiNO_3$ mixture. The effect of advanced surfaces on the performance of a tubular absorber is analysed through the comparison of these results with those obtained with a smooth tube. Both advanced surface tubes and smooth tubes have an exterior diameter of 8.0 mm and a length of one metre. Results were achieved at a cooling-water temperature of 40 ºC.

Fig. 3a depicts the NH_3 absorption mass flux values for both advanced and smooth surface tubes with cooling-water flows in low transition and turbulent regimes. For the transition regime, we found that the absorption mass flux increased from 0.0037 to 0.0061 $kg.s^{-1}m^{-2}$ when the solution mass flow in the advanced surface tube was changed from 20 to 70 $kg.h^{-1}$. In the case of the smooth tube, the corresponding values were between 0.0032 and 0.0035 $kg.s^{-1}m^{-2}$ at the same operating conditions. When a turbulent regime in the cooling-water flow was set, the absorption mass flux for the advanced surfaces increased from 0.0048 to 0.0080 $kg.s^{-1}m^{-2}$ when the solution mass flow was changed from 20 to 60 $kg.h^{-1}$. Moreover, the corresponding values for the smooth tube increased from 0.0036 to 0.0055 $kg.s^{-1}m^{-2}$. It should be noted that the absorption mass flux achieved with the advanced surface tube was even higher than the values reported by Oronel et al. [17] with a corrugated plate heat exchanger as the absorber. At the same operating conditions for turbulent regime, the absorption mass flux using the advanced surface tube was approximately twice as high as the values achieved with the corrugated plate heat exchanger. Infante Ferreira [16] also conducted an experimental study with a tubular bubble absorber with an $NH_3/LiNO_3$ mixture and four different smooth tubes with internal diameters of 10, 15.3, 20.5 and 25.7 mm. The author reported a maximum absorption mass flux of 0.0038 $kg.s^{-1}m^{-2}$ with a 10 mm internal diameter smooth tube, but the operating conditions were quite different. Although the solution inlet temperature and concentration were quite similar, solution

flow rates were much higher while the absorber pressure and inlet cooling-water temperature were lower.

Results for the heat transfer coefficients with cooling-water flow in fully developed turbulent regime are not shown because of their high uncertainty propagation due to the insignificant increase in the cooling-water temperature. Our experiments show that for cooling-water flows in a low transition regime, the maximum potential in the absorption mass flux is not reached if compared with results for a fully developed turbulent flow. Although the thermal resistance was dominant in the solution side rather than in the water side in all our experiments, increasing the water side heat transfer coefficient also increased the absorption mass flux. The same behaviour was observed by Cerezo et al. [15, 24] with an NH_3/H_2O mixture and Oronel et al. [17] with an $NH_3/LiNO_3$ mixture, both using a plate heat exchanger as an absorber. In general terms, the absorption mass flux values in the advanced tube represent a significant improvement over the values achieved with the smooth tube. For instance, at low cooling-water Reynolds numbers and solution mass flows of 40 and 50 $kg.h^{-1}$, the absorption mass fluxes in the advanced surface tube were 1.46 and 1.57 times higher than the values achieved for the smooth tube. At high cooling-water Reynolds numbers, the absorption mass fluxes of the advanced surface tube were 1.71 and 1.54 times higher than the values achieved with the smooth tube.

Fig. 3b shows the solution heat transfer coefficient as a function of the solution mass flow rate at low cooling-water flows. As mentioned earlier, solution heat transfer coefficients for high cooling-water flows are not shown because the uncertainty propagations were high for the absorber thermal load and were therefore also high for the solution heat transfer coefficients. However, Fig. 3b shows that the solution heat transfer coefficient increased from 1.24 to 2.55 $kW.m^{-2}K^{-1}$ when the solution mass flow in the advanced surface tube was changed from 20 to 70 $kg.h^{-1}$. On the other hand, the solution heat transfer coefficient in the smooth tube increased only slightly, from 1.13 to 1.64 $kW.m^{-2}K^{-1}$. The solution heat transfer coefficient values from the advanced surfaces were 1.11 and 1.55 times higher than the values from the smooth surfaces when the solution mass flow rate was set between 40 and 70 $kg.h^{-1}$. Interestingly, the low Reynolds numbers established for the cooling-water limited the improvement of the solution heat transfer coefficients in relation to the solution mass flow. Contrary to what was seen with the absorption mass flux, the solution heat transfer coefficients obtained with the advanced surface tubes in our study were lower than those obtained by Oronel

et al. [17] with the corrugated plate heat exchanger absorber. This difference in behaviour may be related to the deficient use of the tube area in the heat transfer process. Infante Ferreira [16] obtained a maximum value of 2.53 $kW.m^{-2}K^{-1}$ for the solution heat transfer coefficient with a 10 mm inner tube diameter.

Fig. 3c shows the mass transfer coefficient as a function of the solution mass flow. As expected, mass transfer coefficients seem to show a similar trend to absorption mass flux. At low cooling-water Reynolds numbers and solution mass flows between 20 and 70 $kg.h^{-1}$, the mass transfer coefficient in the absorber with the advanced surface tube increased from 1.49 to 1.85 $m.h^{-1}$, while mass transfer coefficients using the smooth tube were around 1 $m.h^{-1}$. Moreover, when turbulent cooling-water regimes were set, mass transfer coefficients increased from 1.56 to 2.58 $m.h^{-1}$ and from 1.1 to 1.7 $m.h^{-1}$ in the advanced and smooth surface tubes, respectively. While the results obtained with the smooth tube at low cooling-water Reynolds numbers were similar to those obtained by Oronel et al. [17] with the corrugated plate heat exchanger, the results obtained with the advanced surface tube and turbulent cooling-water regime were 2.5 times higher. The maximum value reported by Infante Ferreira [16] was 0.79 $m.h^{-1}$ in this case with a 20.5 mm inner tube diameter.

It was expected that the advanced surfaces predominantly enhance heat transfer; however we found that the use of advanced surfaces in the configurations studied enhanced mass transfer more than heat transfer. These greater improvements in mass transfer were probably due to the fact that advanced surfaces not only act as turbulators. The centrifugal effect of helical micro-fins may also force the bubbles into contact with the rough and micro-finned walls, making the ammonia bubbles break more easily and, therefore, absorb more easily.

The subcooling degree of the solution leaving the absorber in all our case studies increased when the solution mass flow was changed from 10 to 70 $kg.h^{-1}$, as shown in Fig. 3d. The figure also shows that subcooling in the absorber with advanced surfaces yields slightly lower values than with a smooth tube. All subcooling values obtained were below 5 ºC, which indicates that the tested absorbers operated near optimal performance for the selected operating conditions.

4.2 Effect of the tube diameter

The effect of the tube diameter on NH_3 absorption mass flux, mass transfer coefficient, degree of subcooling and solution concentration difference is depicted in Fig. 4 for 1 m length absorber. Studies were conducted using two advanced surface tube diameters (9.5 mm and 8 mm, OD) at an inlet cooling-water temperature of 40 ºC and cooling-water flows in a turbulent regime.

Fig. 4a and 4c show that higher absorption mass fluxes were achieved when the tube diameter was reduced from 9.5 mm to 8.0 mm. The maximum NH_3 absorption mass flux obtained with the 9.5 mm tube diameter was 0.0059 $kg.s^{-1}m^{-2}$, while 0.008 $kg.s^{-1}m^{-2}$ was achieved with the smaller tube diameter. Fig. 4b shows that mass transfer coefficients range from 1.2 to 2.6 $m.h^{-1}$ and from 1.0 to 1.4 $m.h^{-1}$ for tubes with diameters of 8.0 mm and 9.5 mm, respectively.

The subcooling degree values are presented in Fig. 4d. The degree of subcooling of the solution leaving the absorber was lower when a tube with a diameter of 8.0 mm was used. The maximum value obtained in the tube with a diameter of 9.5 mm was approximately 5.9 ºC. The results for heat transfer performance are not presented here for the reasons laid out in sub-section 4.1.

The experimental results described in this sub-section indicate that, as expected, the higher solution and ammonia vapour velocities achieved by reducing the tube diameter result in an increase in mass transfer rate. However, the increased mass transfer rate was offset by the reduction in transfer area, resulting in a similar absorption capacity for both tubes. Our results are in good agreement with the experimental data reported by Infante Ferreira [16].

4.3 Effect of the tube length

We performed an experimental characterisation of an $NH_3/LiNO_3$ tubular absorber with advanced surface tube of 8.0 mm (OD) and two tube lengths (1 and 3 metres) under differing operating conditions of solution mass flow rate and cooling-water temperature.

Fig. 5 shows the effect of the absorber length on the absorption mass flux and thermal load in the absorber, with the cooling-water temperature set at 40 ºC and 35 ºC. Fig. 5a shows that absorption mass flux values decreased when the length of the tube absorber was increased to three metres instead of one metre. Therefore, although we achieved a

considerable increase in the thermal load, the improvement of the thermal load was not proportional to the increase in tube length. We also found that the absorption mass flux tended to gradually decrease for solution mass flow rates over 40 $kg.h^{-1}$ in the three-metre absorber.

Fig. 6a shows that solution heat transfer coefficients range from 1.10 to 1.80 $kW.m^{-2}K^{-1}$, and from 1.80 to 3.10 $kW.m^{-2}K^{-1}$ for the one- and three-metre absorbers, respectively, when the solution mass flow was increased from 10 to 60 $kg.h^{-1}$ and the cooling-water temperature was set to 40 ºC. Therefore, higher solution heat transfer coefficients were achieved with the three-metre absorber. Although the increase in the thermal load was lower than the increase in the heat transfer area with the three-metre absorber, the LMTD of this absorber was much lower than that of the one-metre absorber (Fig. 6b). The reason for this trend is that less vapour is absorbed in the final section of the absorber and therefore less absorption heat is dissipated. This allows the solution to be cooled to close to the coolant inlet temperature.

Fig. 7a illustrates the effect of the length of the advanced surface tube on the mass transfer coefficient. As the figure shows, mass transfer coefficient values followed a more uneven trend compared to the absorption mass flux results, although the values for the one-metre tube absorber remained higher. Finally, Fig. 7b displays the subcooling degree of the solution leaving the absorber. All of the values achieved were below 5 ºC, which indicates that the absorber was operated near its maximum efficiency at the operating conditions established.

4.3 Total pressure drop

One would expect that the insertion of micro-fins in a plain tube would also give rise to a drop in pressure in the absorber and thereby reduces absorber pressure and thus absorption capacity. The effect of the micro-fin wire on pressure drop rates was therefore investigated. Fig. 8 shows the experimental pressure drops in the plain tube absorber and in the micro-finned tube absorber of 1m length as a function of solution mass flow rate. The pressure drops in the smooth and advanced surface tube are similar. Therefore, for the operating conditions considered in this work, the advantage of using micro-finned tubes for bubble absorbers is clearly justified, as they enhance heat and mass transfer processes without penalising pressure.

5. Conclusions

This work studies the intensification of heat and mass transfer processes with the use of advanced surfaces in an $NH_3/LiNO_3$ tubular bubble absorber. We conducted a performance comparison of an absorber using advanced and smooth surfaces. The operating conditions set for the experiments were those of interest for absorption chillers driven by low-temperature heat sources. Our results allow us to draw the following conclusions:

- Experimental data showed that advanced surfaces significantly improve the absorption process in the tubular bubble absorber compared to using a smooth tube. The effect of the advanced surface tubes was greater when the solution mass flow was increased. At low cooling-water Reynolds numbers and solution mass flow rates of 40 and 50 $kg.h^{-1}$, absorption mass fluxes for the tube with advanced surfaces were approximately 1.46 and 1.57 times higher than the values achieved with the smooth tube. At high cooling-water Reynolds numbers, absorption mass flux values for the tube with advanced surfaces were approximately 1.71 and 1.54 times higher than those achieved with the smooth tube.
- Improvements in the solution heat transfer coefficient were also obtained with advanced surfaces. These improvements, more pronounced at high solution mass flows, were approximately 1.11 and 1.55 times higher than the values achieved with the smooth surface when the solution mass flow rate was set between 40 and 70 $kg.h^{-1}$.
- Geometric parameters, such as tube diameter and tube length, are essential in absorber design. We analysed absorber performance with two internal micro-finned tube diameters and two lengths. Our experimental results showed that the absorption mass flux increased when the tube diameter was decreased and decreased when the tube length was increased. However, the larger area of the tube with the higher diameter allows the absorber's thermal load to be maintained. On the other hand, increasing the tube length results in a significant increase in the absorption capacity, but in a smaller proportion to the increase in area.
- Micro-finned tubes increase heat and mass transfer coefficients without penalising absorber pressure.

Acknowledgements

This study is part of an R&D project funded by the Spanish Ministry of Science and Innovation (ENE2008-00863). The authors would like to thank HYDRO for providing the advanced surface tubes. Carlos Amaris would like to thank the Spanish Ministry of Science and Innovation for the award of his scholarship (BES-2009-015241).

References

[1] K. Gensch, Lithiumnitratammoniakat als absorptionsflüssigkeit für kältemaschinen, Zeitschrift für die gesamte Kälte, Industrie, 2 (1937) 24–30.

[2] M.K. Aggarwal, R.S. Agarwal, Thermodynamic properties of lithium nitrate ammonia mixtures, International Journal of Energy Research 10(1) (1986) 59-68.

[3] C.A. Infante Ferreira, Thermodynamic and physical property data equations for ammonia-lithium nitrate and ammonia-sodium thiocyanate solutions, Solar Energy 32 (2) (1984) 231-236.

[4] K.A. Antonopoulos, E.D. Rogdakis, Performance of solar driven ammonia-lithium nitrate and ammonia-sodium thiocyanate absorption systems operating as coolers or heat pumps in Athens, Applied Thermal Engineering 16 (2) (1996) 127-147.

[5] D.W. Sun, Comparison of the performances of NH_3-H_2O, NH_3-$LiNO_3$ and NH_3-NaSCN absorption refrigeration systems, Energy Conversion Management 39 (1998) 357-368.

[6] J.M. Abdulateef, K. Sopian, M.A. Alghoul, Optimum design for solar absorption refrigeration systems and comparison of the performances using ammonia water, ammonia-lithium nitrate and ammonia-sodium thiocyanate solutions, International Journal of Mechanical and Materials Engineering 3 (1) (2008) 17-24.

[7] C.A. Infante Ferreira, Operating characteristics of NH_3-$LiNO_3$ and NH_3-NaSCN absorption refrigeration machines, Proceedings of The Nineteenth International Congress of Refrigeration, vol. IIIa, 1995, 321-328.

[8] R. Ayala, J.L. Frías, C.L. Heard, F.A. Holland, Experimental assessment of and ammonia/lithium nitrate absorption cooler operated on low temperature geothermal energy, Heat Recovery Systems & CHP 14 (1994) 437-446.

[9] C.L. Heard, R. Ayala, R. Best, An experimental comparison of an absorption refrigerator using ammonia/water and ammonia/lithium nitrate, Proceedings of the International Sorption Heat Pump Conference, Montreal, Canada, 1996, 245-252.

[10] J-K. Kim, C.W. Park, Y. T. Kang, The effect of micro-scale surface treatment on heat and mass transfer performance for a falling film H_2O/LiBr absorber, International Journal of Refrigeration 36 (2003) 575-585.

[11] W.A. Miller, The synergism between heat and mass transfer additive and advanced surfaces in aqueous LiBr horizontal tube absorbers, Proceedings of the International Sorption Heat Pump Conference, Munich, Germany,1999.

[12] C.W. Park, H.C. Cho, Y.T. Kang, The effect of heat transfer additive and surface roughness of micro-scale hatched tubes on absorption performance, International Journal of Refrigeration 27 (2004) 264-270.

[13] Y. T. Kang, A. Akisawa, T. Kashiwagi, Experimental correlation of combined heat and mass transfer for NH_3–H_2O falling film absorption, International Journal of Refrigeration 22 (1999) 250–262.

[14] K. B. Lee, B. H. Chun, J. C. Lee, C. H. Lee, S. H. Kim, Experimental analysis of bubble mode in a plate-type absorber, Chemical Engineering Science 57 (2002) 1923 – 1929.

[15] J. Cerezo, M. Bourouis, M. Valles, A. Coronas, R Best, Experimental study of an ammonia–water bubble absorber using a plate heat exchanger for absorption refrigeration machines, Applied Thermal Engineering 29 (2009) 1005–1011.

[16] C.A. Infante Ferreira, Vertical tubular absorbers for ammonia-salt absorption refrigeration, PhD thesis, Delft Technical University, Delft, 1985.

[17] C. Oronel, C. Amaris, M. Bourouis, M. Vallès., Heat and mass transfer in a bubble plate absorber with $NH_3/LiNO_3$ and $NH_3/(LiNO_3+H_2O)$ mixtures, International Journal of Thermal Sciences 63 (2013) 105-114.

[18] S. Libotean, D. Salavera, M. Valles, X. Esteve, A. Coronas, Vapour-liquid equilibrium of ammonia + lithium nitrate + water and ammonia + lithium nitrate solutions from (293.15 to 353.15) K, Journal of Chemical and Engineering Data 52 (2007) 1050-1055.

[19] S. Libotean, A. Martin, D. Salavera, M. Valles, X. Esteve, A. Coronas, Densities, viscosities, and heat capacities of ammonia + lithium nitrate and ammonia + lithium nitrate + water solutions between (293.15 and 353.15) K, Journal of Chemical and Engineering Data 53 (10) (2008) 2383-2388.

[20] V. Gnielinski, New equations for heat and mass transfer in turbulent pipe and channel flow, International Chemical Engineering 16 (1976) 359–368.
[21] B.S. Petukhov, Heat transfer and friction in turbulent pipe flow with variable physical properties, Advances in Heat Transfer 6 (1970) 503-564.
[22] B. S. Petukhov and L. I. Roizen, Generalized Relationships for Heat Transfer in a Turbulent Flow of a Gas in Tubes of Annular Section, High temperature (USSR) 2 (1964) 65–68.
[23] B.N. Taylor, C.E. Kuyatt, Guidelines for Evaluating and Expressing the Uncertainty of NIST Measurement Results, National Institute of Standards and Technology Technical Note 1297, 1994.
[24] J. Cerezo, R. Best, M. Bourouis, A. Coronas, Comparison of numerical and experimental performance criteria of an ammonia–water bubble absorber using plate heat exchangers, International Journal of Heat and Mass Transfer 53 (2010) 3379–3386.

Table 1. Geometric specifications of the tubular absorber.

Specifications	Value		
Advanced surface tube Manufacturer	Hydro		
Absorber length, m	1.0		3.0
Heat exchange area, m^2	0.029	0.025	0.076
Internal hydraulic diameter, m	0.0075	0.006	0.006
Annular hydraulic diameter, m	0.0035	0.005	0.005
Fin length, m	0.0003		

Table 2. Uncertainty values of the measured and calculated parameters.

Parameters	Uncertainty
Sensors	
Temperature, T (ºC)	± 0.1
System pressure, P (Bar)	± 0.25 %
Solution mass flow rate, m_S ($kg.h^{-1}$)	± 0.1 %
Solution density, ρ_S ($kg.m^{-3}$)	± 0.5
Cooling water flow rate, V_{Cw} ($l.h^{-1}$)	± 0.24
Tubular Absorber	
Tube diameter, mm	0.02
Tube length	± 0.5 %
Calculated parameters	
Δx	8.1 %
NH_3 absorption mass flux, F_{AB}	5.7 %
Solution heat transfer coefficient, h_S	13.4 %
Solution mass transfer coefficient, K_m	11.2 %

Table 3. Operating conditions of the experimental study.

Parameters	Range
Solution temperature at the absorber inlet, °C	45
Cooling-water temperature at the absorber inlet, °C	35.0-40.0
Ammonia mass fraction of the solution at the absorber inlet	0.452
Absorber pressure, kPa	510
Solution mass flow rate, kg/h	10.0-72.0
Cooling-water flow rate in the tubular absorber, l/h	80-435

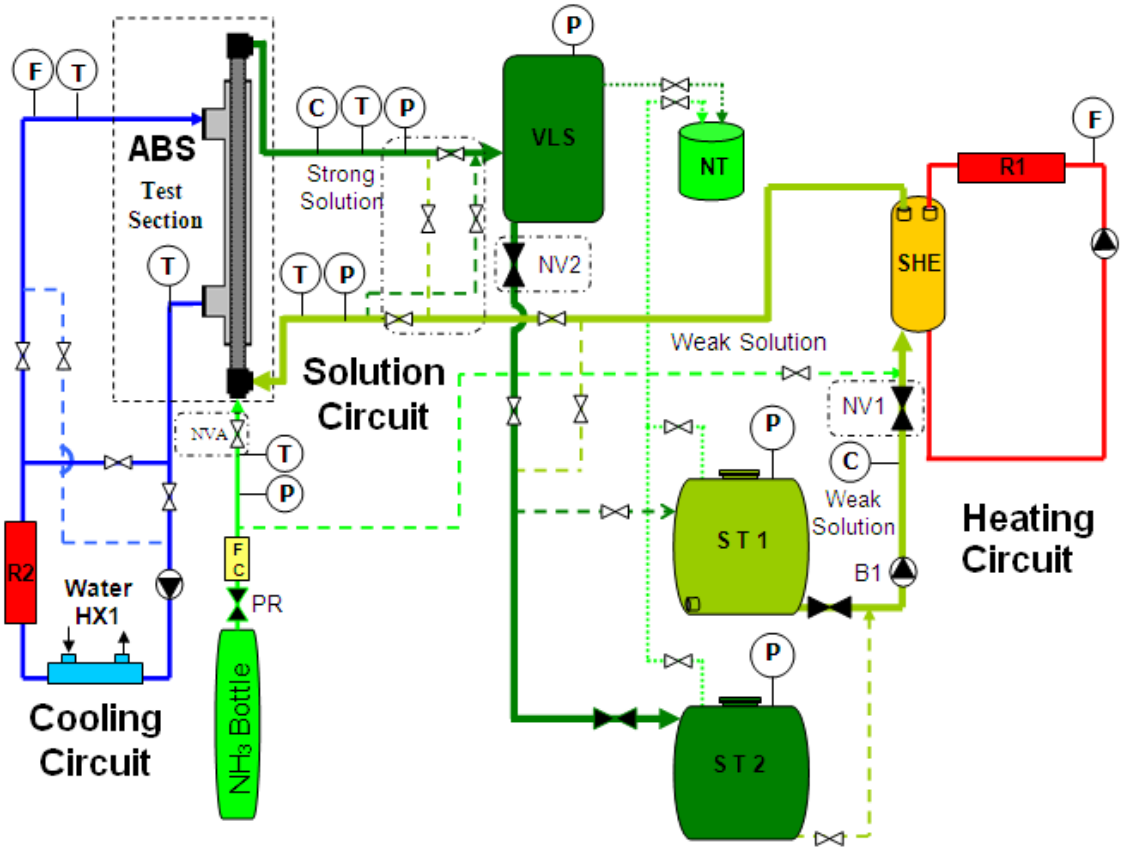

Figure 1. Schematic of the experimental test facility.

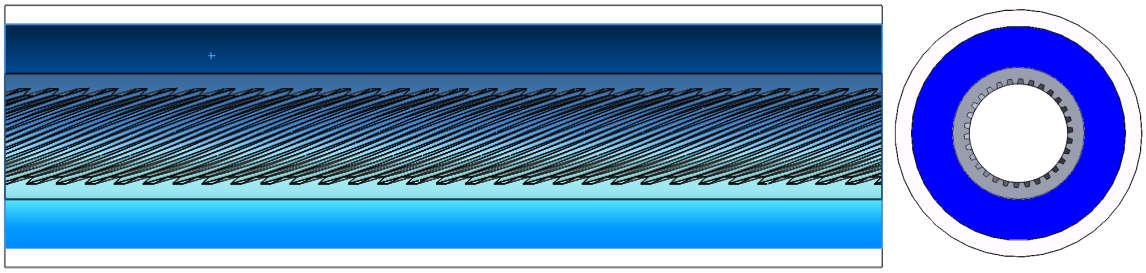

Figure 2. Cross-section view of the advanced surface tube.

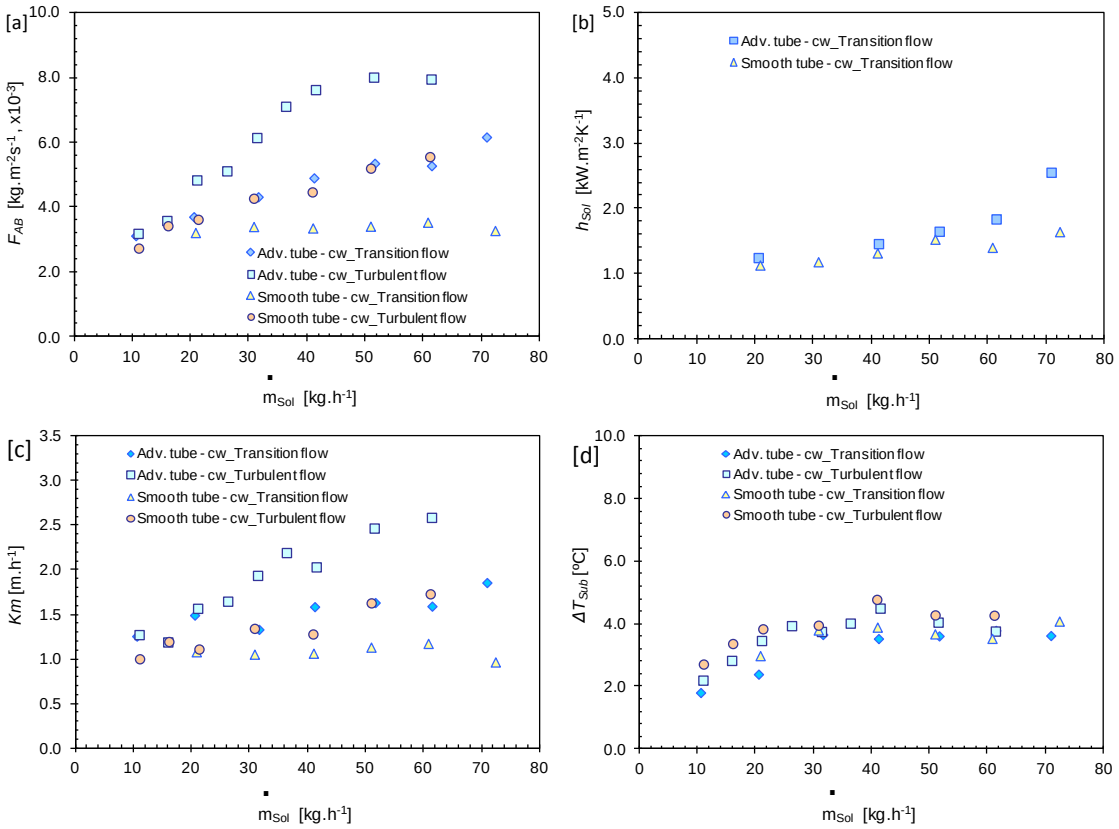

Figure 3. Effect of advanced surfaces for 1 m length absorber and OD tube diameter of 8mm on: [a] NH_3 absorption mass flux, [b] solution heat transfer coefficient, [c] mass transfer coefficient and [d] degree of subcooling.

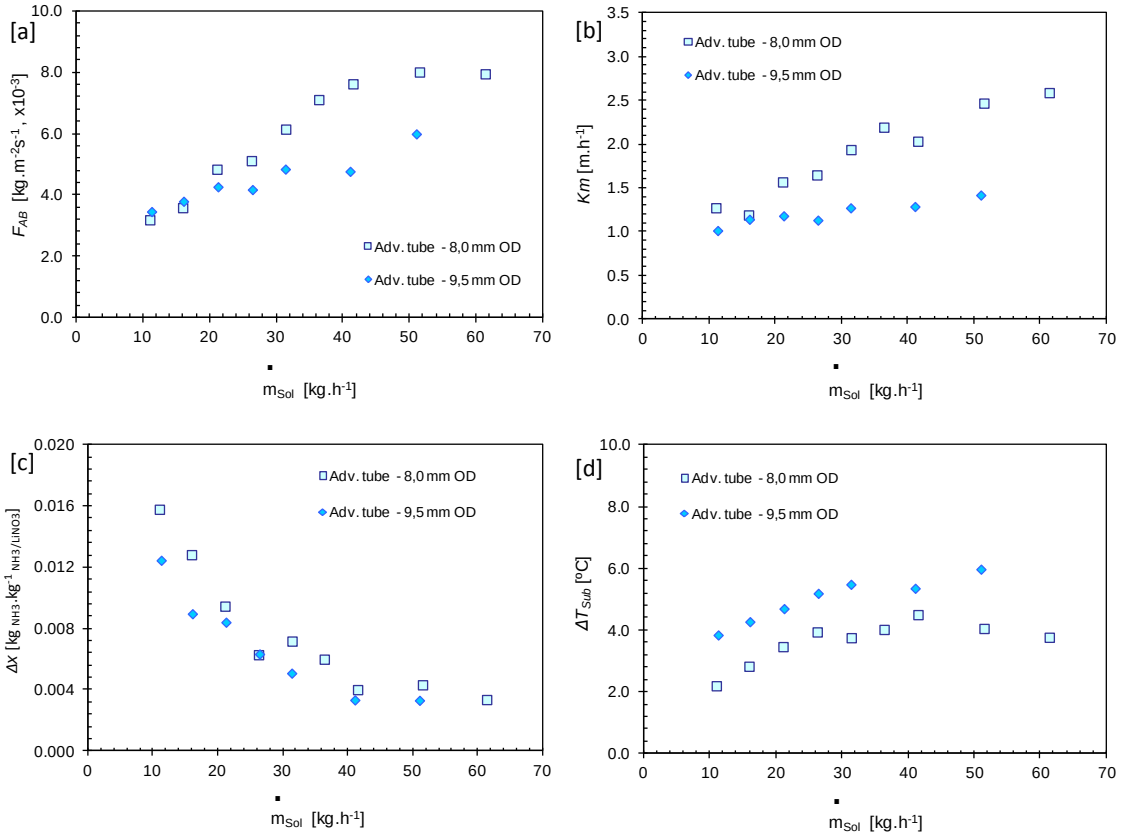

Figure 4. Effect of the advanced surface tube diameter: [a] NH_3 absorption mass flux, [b] mass transfer coefficient, [c] solution concentration difference, and [d] degree of subcooling.

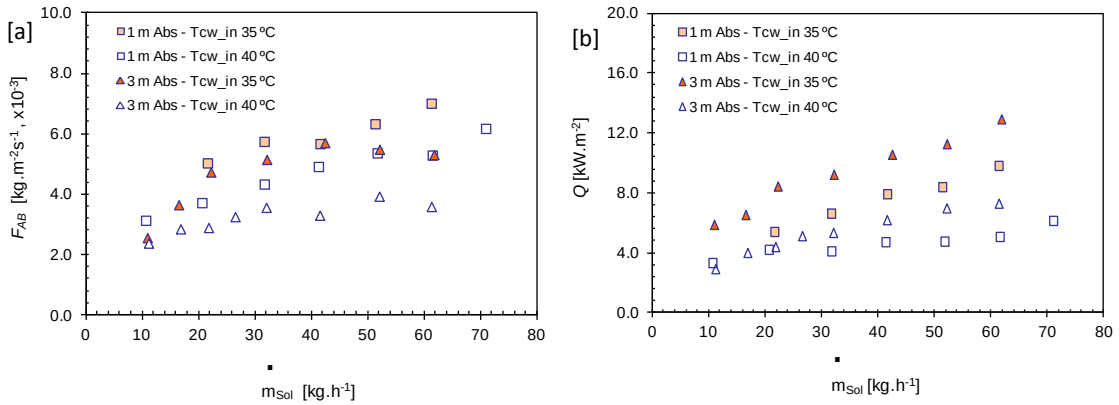

Figure 5. Effect of the advanced surface tube length on: [a] NH_3 absorption mass flux, and [b] thermal load.

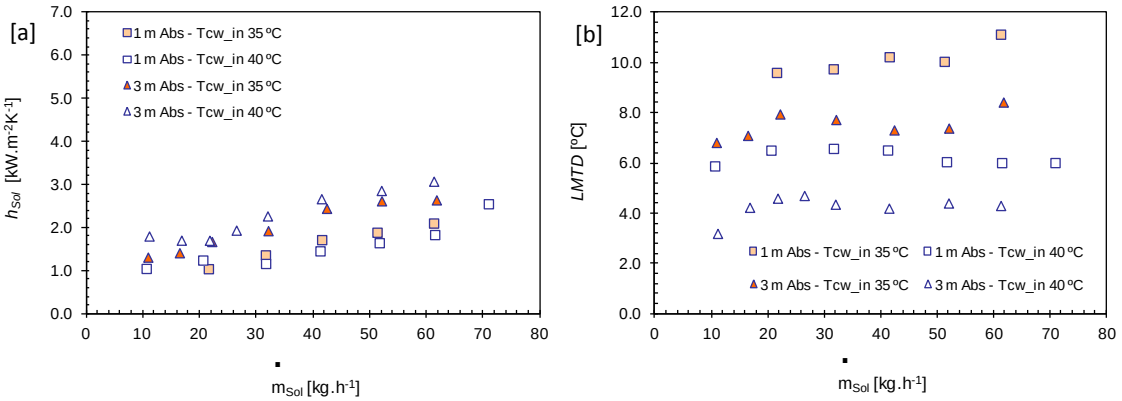

Figure 6. Effect of the advanced surface tube length on: [a] solution heat transfer coefficient, and [b] LMTD.

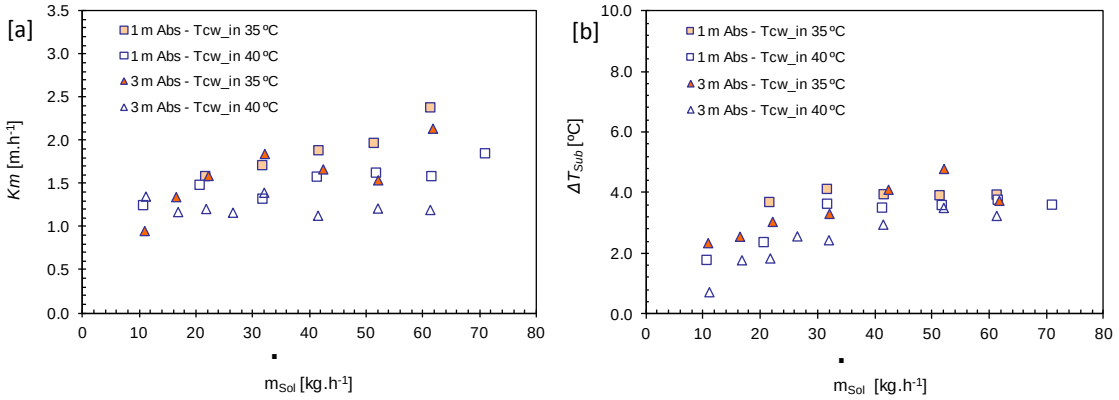

Figure 7. Effect of the advanced surface tube length on: [a] mass transfer coefficient, and [b] degree of subcooling.

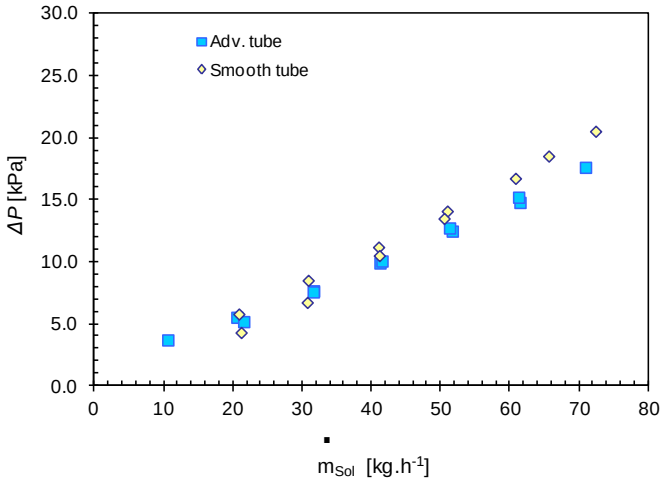

Figure 8. Total pressure drop in the absorber of 1 m length with and without advanced surfaces.